JOURNAL OF SOLID STATE CHEMISTRY 105, 520–527 (1993)

Ionic Displacements and Piezoelectric Constants of $AgGaS_2$ from X-Ray Diffraction of a Crystal in an External Electric Field

HEINZ GRAAFSMA* AND PHILIP COPPENS

Chemistry Department, State University of New York at Buffalo, Buffalo, New York 14214

AND JAROSLAW MAJEWSKI AND DAVID CAHEN

Department of Materials and Interfaces, Weizmann Institute of Science, Rehovot 76100, Israel

Received July 29, 1992; in revised form December 28, 1992; accepted December 30, 1992

The displacements of the ions and the changes in cell parameters which occur on application of an electric field to a crystal of $AgGaS_2$ have been determined using X-ray diffraction. The shifts in Bragg angle of 14 reflections, due to a field of 2.6×10^6 V/m applied nearly parallel to [221], were used to refine the change in cell parameters. The resulting piezoelectric coefficients are $d_{14} = d_{25} = 8.8$ (0.9) $\times 10^{-12}$ C/N and $d_{36} = 7.6$ (1.8) $\times 10^{-12}$ C/N. This leads to a value of 4.8 (0.5) $\times 10^{-12}$ pC/N for the piezoelectric constant in the [221] direction, which compares well with a value of 5–6 $\times 10^{-12}$ C/N measured directly. The ionic displacements were studied for two field directions. With $E = 2.6 \times 10^6$ V/m in a direction parallel to [110], very small, but significant **a** and **b** direction displacements were observed for all atoms, whereas the displacements in the **c** direction were negligible as expected. Relative to the sulfur framework, the Ga ion displacement is considerably larger than that of the Ag ions. The changes in scattering intensity for a field parallel to [221] were found to be much smaller, indicating smaller ionic displacements for that field direction. The ion displacements are analyzed with a model of nonpolarizable harmonic oscillators in an electric field. It is found that the observed displacements of the Ga ions are much larger than the calculated displacements, whereas the displacements of the Ag ion are in good agreement with theory.

Introduction

With the development of more powerful rotating-anode and synchrotron X-ray sources it has become possible to study bulk physical properties such as the piezoelectric effect on a microscopic scale, allowing a more fundamental understanding of these processes at the atomic level. In particular, techniques which measure *changes* in diffracted intensities and Bragg angles upon external perturbation are highly sensitive and less prone to systematic errors.

In a previous study we measured the reorientation of the molecule 2-methyl-4-nitroaniline in an applied electric field (*1*). We describe here an X-ray diffraction study of the influence of an external electric field on single crystals of $AgGaS_2$. $AgGaS_2$ is a member of the $A^IB^{III}C^{VI}_2$ family of compounds with chalcopyrite structure. It is piezoelectric (*2*) and shows nonlinear optical properties (*3*, *4*). In addition it is a mixed ionic–electronic conductor with predominant ionic conductivity (*5*, *6*). A preliminary account of this work has been published (*7*).

* Present address: European Synchrotron Radiation Facility, B.P. 20, 38043 Grenoble Cedex, France.

0022-4596/93 $5.00

Theory

When a strong electric field is applied to a noncentrosymmetric crystal, homogeneous deformation of the crystal occurs. A homogeneous deformation can be described as having two components (*8*). The displacement of a particle k in unit cell m may be written as

$$u_i(k, m) = u_i(k) + \sum_j U_{ij} x_j(k, m), \quad (1)$$

where $\mathbf{u}(k)$ is a displacement vector identical for all particles k in different unit cells, U_{ij} are the elements of a deformation tensor, and $\mathbf{x}(k, m)$ is the position vector of particle k in unit cell m with respect to a *fixed* origin. The second term on the right hand side of Eq. (1) corresponds to a change in cell parameters and correspondingly to a change in crystal shape. It describes an elastic deformation of the crystal, and is referred to as the *elastic* or *external* strain. In the X-ray diffraction experiment, this external strain causes a change in Bragg angle of the reflections, but in the case of atomic or monatomic ionic solids it has little influence on the scattering intensities. This is because, in the absence of rigid polyatomic units, external strain does not change the fractional coordinates of the atoms when referred to the new basis. Therefore, the exponent in the structure factor equation

$$F_{\mathbf{H}} = \sum_j f_j \exp\{2\pi i \sum_k (h_k x_{jk})\} T_j \quad (2)$$

is invariant, and $F_{\mathbf{H}}$ changes only through small changes in atomic scattering factors f_j, via the change in $\sin\theta/\lambda$, and possible changes in the temperature factors T_j.

The first term of Eq. (1) does not involve a cell deformation, since the displacements of equivalent atoms are the same for all unit cells, irrespective of their distances from the fixed origin. The term represents the displacements of each of the atoms within the deformed unit cell, and is referred to as the *internal* strain. In contrast to the external strain, it does not affect the Bragg angle of the reflections but gives a much larger change in scattering intensity, since now the fractional coordinates of the atoms and correspondingly the exponent in the structure factor will change.

In summary, in the case of atomic solids, the external strain can be determined by measuring the changes in Bragg angle of the reflections, and the internal strain by measuring the changes in scattering intensity of the reflections.

Experiment

Sample Preparation

Crystals were obtained from A. Gentile. They were grown from the melt by the Bridgman technique, using the method of Route *et al.* (*9*) as modified by Kyle (*10*). The crystals were oriented by Laue X-ray diffraction and subsequently cut using a wire saw.

Two samples were selected. Crystal #1 had dimensions $0.375 \times 0.675 \times 4.25$ mm; the 0.675×4.25 mm faces were covered with 200 nm of gold by sputtering. A voltage of 1×10^3 V, with a frequency of $\nu = 55.7$ Hz, was applied over the 0.375 mm to give a field of 2.7×10^6 V/m, nearly parallel to the [221] direction. Crystal #2 had dimensions $0.40 \times 0.70 \times 3.0$ m; the 0.7×3.0 mm faces were covered with gold. An electric field of 1×10^3 Volt, with a frequency of 55.4 Hz, was applied parallel to the [110] direction (Fig. 1). With a gap of 0.4 mm this corresponds to 2.5×10^6 V/m.

The crystals were held between two gold plated clamps which served as electrical contacts (Fig. 2), and mounted on a Huber four-circle diffractometer. We note that in this configuration, no ionic conductivity is possible since the contacts are ionically blocking. Current flow was in the μA range.

Data Collection and Data Reduction

Data were collected at a Rigaku rotating anode source with Mo$K\alpha$ radiation and at the SUNY X3 beamline at Brookhaven

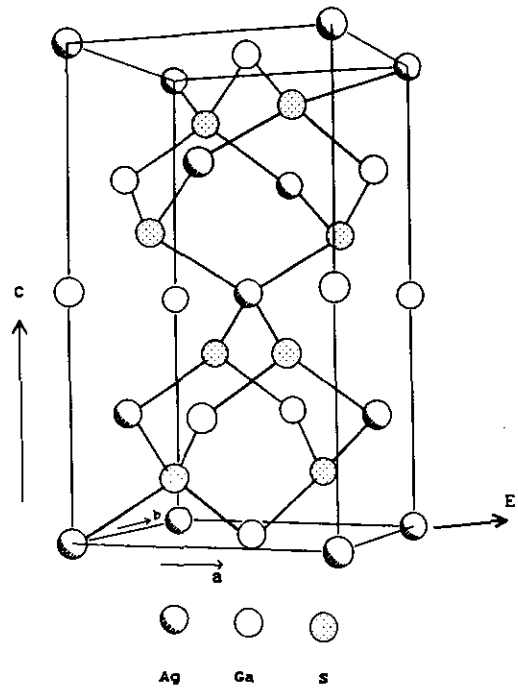

FIG. 1. Unit cell of $AgGaS_2$ with the electric field applied along [110] (sample #2).

National Laboratory with $\lambda = 1.20$ Å photons. To measure both the change in intensity and the change in Bragg angle upon application of the field we use the three-step modulation method (*11*, *12*), which is a modification of earlier modulation methods (*13*, *14*). The electric field is applied to the crystal in three steps (field "up," field "down," and zero field) with a frequency of approximately 50 Hz. The output of the detector is synchronously gated to three different counting chains, such that three different reflection profiles, corresponding to each of the three states of the electric field, are recorded in one single scan.

The change in Bragg angles may be determined by averaging of the shifts of the reflection at the positive and negative θ sides (*15*). The piezoelectric elements can be derived from the Bragg angle changes $\Delta\theta_r$ using the Barsch equation (*16*),

$$\Delta\theta_r = -\tan\theta_r \sum_{i=1}^{3}\sum_{j=1}^{3} h_{r,i}h_{r,j}\varepsilon_{ij} = -E\tan\theta_r \sum_{k=1}^{3}\sum_{i=1}^{3}\sum_{j=1}^{3} e_k h_{r,i}h_{r,j}d_{kij}, \quad (3)$$

where ε_{ij} is the ijth component of the strain tensor ε, d_{kij} the kijth component of the piezoelectric tensor $\mathbf{d}$, and the e_k's and the $h_{r,i}$'s are the direction cosines of the electric field (of magnitude E) and the diffraction vector $\mathbf{h}_r$ respectively. Alternatively the piezoelectric elements can be derived by determination of the complete strain tensor, including a rigid rotation of the lattice, from the change in direction of the scattering vectors relative to a laboratory-based coordinate system (*15*).

The intensity changes are determined by measuring the *response ratios* η,

$$\eta_{\pm 0} = \frac{\Delta I_{\pm}}{I_0} = \frac{I_{\pm} - I_0}{I_0}, \quad (4)$$

where I_+, I_-, and I_0 refer to the intensity with field up, down, or zero respectively. The response ratio η_{+-} is the relative difference between field up and field down scattering, equal to $\eta_{+0} - \eta_{-0}$. Since the three intensities I_+, I_-, I_0 are measured at very small time intervals, virtually all experimental instabilities cancel in the response ratio calculations, thus allowing the measurement of very small intensity changes (<0.05%), as well as small positional shifts of the reflection resulting from the change in cell parameters (*17*).

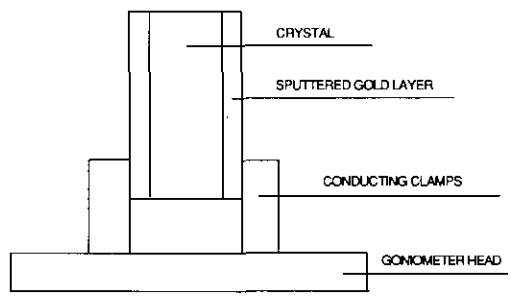

FIG. 2. Schematic drawing of the sample mounting.

To place the intensity changes on an absolute scale, the relative changes were multiplied by $|F_c|^2$ (*14*), where F_c is the calculated structure factor obtained from the known structure, according to

$$\Delta F^2_{+-} = \eta_{+-} F^2_c. \quad (5)$$

Analogous expressions were used for η_{+0} and η_{-0}. The resulting ΔF^2 values are the input for the least-squares refinement using the program TLSBMOL, in which, to account for the converse piezoelectric effect, different sets of cell parameters are used in the intensity calculation for the two states of the field.

The intensity changes are treated with the following formalism (*18*). If the complex structure factor F is written as $A + iB$, the corresponding value of the structure factor of a perturbed system F_+ may be described as

$$F_+ = (A + \Delta A) + i(B + \Delta B). \quad (6)$$

The difference between the intensities with and without the perturbation leads, after application of Lorentz, polarization, and other appropriate corrections factors, to $\Delta F^2 = F^2_+ - F^2$. Substitution of Eq. (6) gives

$$\begin{aligned}\Delta F^2 = F^2_+ - F^2 &= (A + \Delta A)^2 \\ &+ (B + \Delta B)^2 - (A^2 + B^2) \quad (7) \\ &= 2(A\,\Delta A + B\,\Delta B) + (\Delta A)^2 + (\Delta B)^2\end{aligned}$$

or, for small perturbations,

$$\Delta F^2 = 2A\,\Delta A + 2B\,\Delta B. \quad (8)$$

In the chalcopyrite structure, three types of reflections occur (cf. *19*). Reflections with ($hkl/2$) all even or all odd are zinc-blende like, and involve all three types of atoms; those with h, k even and $l/2$ odd or vice versa reflect the anisotropy associated with the deviations of the anion coordinates from the ideal value of $x = 0.25$ ($x = 0.29$, for $AgGaS_2$ (*20*)), and those with $l/2$ odd are reflections that express the ordering in the cation sublattice, i.e., the difference between Ag and Ga scatterers in the present case.

Results

Change in Cell Parameters and the Piezoelectric Tensor

The changes in cell parameters, or external strain, were studied using crystal #1, with the field approximately parallel to the [221] direction. From the orientation matrix (*21*) and the diffractometer setting angles for **E** parallel to the scattering vector, **E** was determined to be along the reciprocal lattice vector $\mathbf{a}^* + 1.49\mathbf{b}^* + 2.29\mathbf{c}^*$. $AgGaS_2$ belongs to the tetragonal space group $I\bar{4}2d$ and has cell parameters $a = b = 5.75722(3)$ Å, $c = 10.3036(2)$ Å (*20, 22*). The piezoelectric tensor has only three nonzero elements, $d_{14} = d_{25}$ and d_{36}. Thus a field along **a**, **b**, or **c** produces only a change in α, β, or γ, respectively (*23*). Since none of the columns in the piezoelectric tensor contains more than one nonzero element, the full piezoelectric tensor can be obtained with just one crystal setting, providing there is an electric field component along **a**, **b**, and **c**. The changes in Bragg angles of 14 reflections were determined by measuring the shifts of the peaks at both positive and negative diffraction angles, and subsequent averaging (*12*). The corresponding changes in cell parameters were obtained by least-squares refinement of the experimental data. The results are given in Table I. As required by

TABLE I

CELL PARAMETERS (Å,°) AND CHANGES IN CELL PARAMETERS (10^{-4} Å, 10^{-3}°) DUE TO THE EXTERNAL FIELD ALONG [221] FROM THE REFINEMENT OF THE SHIFT IN BRAGG ANGLE OF 14 REFLECTIONS

	$E = 0$	Δ
a	5.75722(3)	0.13(0.09)
b	5.75722(3)	−0.10(0.08)
c	10.3036(2)	−0.47(0.19)
α	90	−0.65(0.12)
β	90	−1.17(0.12)
γ	90	−0.68(0.12)
		R_w = 13.9%
		GOF = 1.4

symmetry the changes in length of the axes are zero within 3σ. This also indicates that the nonlinear terms (representing electrostriction) can be neglected in the converse piezoelectric effect. The ratio between the change in α and the change in β, $\Delta\alpha/\Delta\beta = 0.55\ (0.12)$, is within experimental error equal to the ratio E_a/E_b ($=0.67$) between the components of the field along **a** and **b**, in agreement with the tetragonal symmetry.

The changes in Bragg angle were also used to directly refine the piezoelectric tensor. The result are given below:

$$d_{14} = d_{25} = 8.8\ (0.9)\ \text{pC/N}$$
$$d_{36} = 7.6\ (1.8)\ \text{pC/N}.$$

We note that, unless the crystal polarity is known, the signs of these constants are undetermined. The crystal polarity can be determined either by using other physical properties such as the pyroelectric response (*24*), or by measuring sensitive Bijvoet pairs (*25*). In the case of $AgGaS_2$, however, the piezoelectric coefficients were known to be positive (*2*). The experimental results correspond to a value of 4.8 (0.5) pC/N in the [221] direction, in good agreement with the value of 5–6 pC/N measured by conventional methods (*26*).

Ionic Displacements

The ionic displacements were studied with both samples. For crystal #1, 22 reflections were measured at the NSLS X3 beamline at Brookhaven National Laboratory, with the field nearly parallel to the [221] direction; only 5 of the 22 reflections showed a relative change in intensity larger than 3σ, the largest being 0.25%. Crystal #2 showed a much larger effect. The relative changes in intensity of 23 reflections were determined using a Rigaku Ru200 rotating anode source; 14 of the 23 showed a change larger than 3σ, the largest being 0.51%.

Application of the field in the [110] direction destroys the fourfold inversion and the twofold rotation axes, leaving the *d*-glide plane parallel to [110] as the only symmetry element. As a result there are 1 Ag, 1 Ga, and 2 S atoms in the asymmetric unit of the perturbed crystal. Since the perturbed crystal is polar, the coordinates of one atom have to be kept fixed in the refinement of the atomic displacements to define the origin. All shifts obtained are therefore relative to the atom which is fixed. The effect of bond-charge redistribution on the scattering intensity (*27, 28*) is assumed to be negligible, since the data consist of strong, and relatively high order, reflections. Observed and calculated structure factor changes are listed in Table II. The relative effects of the electric field are of comparable magnitude for all three types of reflections.

In Table III, ionic displacements are given for the refinement with one of the sulfur atoms fixed. Small but significant displacements in the x and y directions occur in particular for the Ga atom. The displacements in the z direction are zero within experimental error, as expected since the field has no component along the z direction and the electrostrictive tensor has no component allowing deformation along the z-axis. The gallium atom shows considerably larger displacements relative to the sulfur framework than the silver atom. The relatively large R/R_w values can be ascribed to the limited data set. More accurate results as well as a better fit may be expected with a larger data set and better values of $I/\sigma(I)$. However, data collection times required for this improvement were prohibitive. Because of the small number of data, the temperature factors had to be kept fixed during the refinement.

Discussion

The ionic displacements can be calculated from the bond stretching and bending force constants of the Ag–S and Ga–S bonds with

TABLE II

DIFFERENCE IN F^2 BETWEEN FIELD UP AND FIELD DOWN

h	k	l	F^2_{obs}	ΔF^2_{obs}	ΔF^2_{calc}	$\sigma(\Delta F^2)$
−1	2	5	15.66	−0.63	−0.71	0.17
−5	2	3	22.69	0.15	0.03	0.30
4	−1	−1	27.54	1.33	1.29	0.38
1	−5	6	97.52	5.55	6.38	1.78
1	−2	−1	43.30	0.96	1.50	0.39
1	−5	−6	99.52	−7.80	−6.90	1.62
2	1	3	21.16	−1.29	−1.10	0.18
4	−4	0	131.90	1.94	0.39	4.71
0	−4	−2	13.08	0.56	0.52	0.08
−4	4	4	74.54	−1.42	−0.27	1.32
0	4	−2	14.69	−0.67	−0.73	0.15
4	0	−2	14.69	−0.87	−0.74	0.14
−4	0	−2	13.08	0.64	0.52	0.09
0	−4	2	14.69	−0.62	−0.73	0.11
4	0	2	13.08	0.43	0.52	0.10
−2	−2	−4	122.30	−8.91	−3.79	1.81
1	−2	5	14.94	0.33	0.37	0.11
3	−3	−10	75.29	1.35	1.60	0.76
4	−5	−7	20.82	−0.31	−0.12	0.22
4	−6	−4	72.71	−1.12	0.57	0.97
0	−8	−6	15.58	−0.56	−0.65	0.13
1	−7	−4	17.60	−0.43	−0.27	0.16
3	−6	−1	24.27	−0.87	−1.08	0.31

R factor including unobserved reflections	0.354
Weighted R factor including unobserved reflections	0.245
Goodness of fit = 1.36	

the assumption of a rigid S-framework. Koschel *et al.* derived the force constants by a least-squares fit of a Keating model to the zone-centered phonon spectrum (*29*). The force constants they obtained for the Ag–S and Ga–S bond were 19.7 and 51.9 Nm^{-1}, respectively. The larger force constant for the Ga–S bond is in agreement with the observed thermal motion in the unperturbed structure (*17*), which indicates the average square displacement of the Ag ions to be approximately 2.5 times that of the Ga ions. It also agrees with the statement that, since Ga has a coordination closer to perfect tetrahedral, Ga–S bonds are more oriented and thus stiffer than Ag–S bonds (*30*).

The displacements $\Delta\mathbf{r}$ of an ion are found by solving the matrix equation

$$\mathbf{dF}\cdot\Delta\mathrm{r} = \mathbf{F}(\text{electric}) = q\mathbf{E}, \qquad (9)$$

where the elements of **dF** are given by

$$(dF)_{ij} = \delta F_i/\delta r_j. \qquad (10)$$

F_i is the component of the force in direction i exerted on the displaced particle. The derivatives in (10) are calculated numerically. Taking the ionic charges from the fit of the

TABLE III

IONIC DISPLACEMENTS (10^{-4} Å) DUE TO A FIELD OF 1.10^6 V/m PARALLEL TO [110].

	Δx	Δy	Δz
Ag	−1.4 (0.7)	−2.5 (0.9)	+0.4 (0.6)
Ga	−4.4 (0.9)	−4.7 (0.9)	0.0 (0.8)
S(1)	+0.5 (0.3)	+0.3 (0.6)	+1.7 (0.8)

R_w = 24.5%
GOF = 1.8

Note. Shifts are relative to *S*(2).

Keating model to the spectroscopic results (*25*), $q_{Ag} = 0.95\ |e|$ and $q_{Ga} = 0.75\ |e|$, we find for an electric field of 2.6×10^6 V/m parallel to [110]

$$\Delta r_{Ag} = 1.22 \times 10^{-4}\ \text{Å} \parallel [110]$$
$$\Delta r_{Ga} = 0.39 \times 10^{-4}\ \text{Å} \parallel [110].$$

The displacement of the Ag ion is in good agreement with the experimental result. The observed displacement of the Ga ion, however, is 10 times the calculated value. To explain the displacements in terms of the present model of nonpolarizable charged harmonic oscillators unrealistically large charges on the Ga atoms would be required.

Using the approximations mentioned above, we find the ionic displacements for an electric field parallel to [221] to be smaller by a factor of 1.2 compared to the [110] field direction. This in agreement with the smaller intensity effects for the [221] direction observed in the experiment.

From a model for linear electrooptic effects, based on the bond-charge dielectric theory of Phillips and van Vechten (*31*), the atomic displacement induced by an electric field in a given direction can be estimated. Using data from (*31*) as well as our own measurements of the dielectric constants of $AgGaS_2$, we calculate displacements of $2–5 \times 10^{-4}$ Å for a field of 2×10^6 V/m, which as an average value is in reasonable agreement with the experimental results.

The calculations presented above contain a number of approximations. The Keating model used in the derivation of the force constants describes the phonon spectrum in terms of rigid ions connected by springs (*32*). Since the ions are assumed to be rigid, polarization effects are neglected. A much more sophisticated model is the Breathing-Shell Model (BSM) (*33*), which has proven successful in lattice dynamics calculations of silver halides (*34*). However, the BSM has to our knowledge not been applied to the phonon spectrum of $AgGaS_2$.

The influence of polarization of the ions on the experimentally observed shifts may be small, as shown by the following argument. Using the polarizibility of Ag, $\alpha(Ag^+) = 1.66 \times 10^{-40}$ Cm²/V (*35*), we obtain with a field of $2.6 \times 10^{+6}$ V/m an induced dipole of 4.31×10^{-34} Cm (1.31×10^{-4} D). This corresponds to an apparent displacement of the total electron cloud of 46 electrons (relative to the nucleus) of 0.59×10^{-6} Å. For Ga^+, $\alpha(Ga) = 3.35 \times 10^{-40}$ Cm²/V (*35*), the corresponding value is 1.75×10^{-6} Å. These displacements are two orders smaller than the observed shifts.

On the other hand, polarization of the ions may also influence the force constants between the ions. Furthermore, these force constants will be affected directly by the external electric field. To get an estimate of the importance of these effects and to clarify the reason for the discrepancy between experiment and calculation it will be necessary to get more accurate data on $AgGaS_2$. This would allow simultaneous refinement of ionic displacements and structural and thermal parameters. In the present study, synchrotron radiation could not be used effectively because deadtime limitations in the counting equipment did not allow use of the full beam intensity. Use of faster counting equipment may eliminate this limitation.

Summary

We have determined the piezoelectric tensor of $AgGaS_2$ by X-ray modulation methods. The obtained tensor gives results which compare well with direct measurements of the piezoelectric coefficient in the [221] direction. The ionic displacements on application of an electric field have also been determined. For an electric field parallel to [110], the Ga atoms showed significantly larger displacements than the Ag atoms, relative to the S framework. This is at variance with the force constants of the Ag–S and Ga–S bonds. For a field nearly parallel to [221] much smaller ionic displacements are observed.

Acknowledgments

Support of this work in the USA by the National Science Foundation (Grant CHE9021069) is gratefully

acknowledged. The SUNY X3 Beamline at NSLS is funded by the Division of Basic Energy Sciences of the U.S. Department of Energy (DEFG0291ER45231). The National Synchrotron Light Source is supported by the U.S. Department of Energy, Division of Materials Sciences and Division of Chemical Sciences. In Rehovot, this work was supported by the Basic Research Foundation, administered by the Israel Academy of Sciences and Humanities, and by the US–Israel Binational Science Foundation, Jerusalem, Israel. We thank Professor R. E. Newnham of Pennsylvania State University for the piezoelectric constant measurement, Dr. A. Gentile of Hughes Research for supplying the crystals of $AgGaS_2$, and Y. Halfon for technical assistance.

References

1. H. Graafsma, A. Paturle, and P. Coppens, *in "ACA Abstracts, Series II," p. 57 (1990).*
2. S. C. Abrahams, R. L. Barns, J. L. Bernstein, and E. H. Turner, *Solid State Commun.* **15,** 737 (1974).
3. G. D. Boyd, H. M. Kasper, and J. H. McFee, *IEEE J. Quantum Electron.* **QE-7,** 563 (1971).
4. D. S. Chemla, P. J. Kupecek, D. S. Robertson, and R. C. Smith, *Opt. Commun.* **3,** 2a (1971).
5. H. M. Kasper, B. Tell, and S. Wagner, U.S. Pat. 4, 115, 633 (1976); B. Tell, S. Wagner, and H. M. Kasper, *J. Electrochem. Soc.* **124,** 536 (1977).
6. E. E. Hellstrom and R. A. Huggins, *J. Solid State Chem.* **35,** 207 (1980).
7. H. Graafsma, J. Majewski, D. Cahen, and P. Coppens, *in* "Materials Research Society Symposium Proceedings," *Solid State Ionics* **210,** 639–643 (1991).
8. M. Born and K. Huang, "Dynamical Theory of Crystal Lattices," pp. 134. Oxford Univ. Press, New York (1954).
9. R. K. Route, R. J. Raymakers, and R. S. Feigelson, *J. Cryst. Growth* **29,** 125 (1975).
10. N. R. Kyle, Final report ASDP, DARPA/AFSD, Contract F04701-76-C-0174 (1982).
11. A. Paturle, H. Graafsma, J. Boviatsis, A. Legrand, R. Restori, P. Coppens, Å. Kvick, and R. Wing, *Acta Crystallogr. Sect. A* **45,** FC25 (1989).
12. A. Paturle, Thesis, University of Grenoble, France, (1990).
13. L. Godefroy, These d'Etat, Faculte des Sciences de Paris, Series A, #4037, # d'ordre 4888, (1963).
14. I. Fujimoto, *Acta Crystallogr. Sect. A* **38,** 337 (1982).
15. H. Graafsma, *J. Appl. Crystallogr.* **25,** 372 (1992).
16. G. R. Barsch, *Acta Crystallogr. Sect. A* **32,** 575 (1976).
17. A. Paturle, H. Graafsma, H.-S. Sheu, and P. Coppens, *Phys. Rev. B* **43,** 14,683 (1991).
18. P. Coppens, D. E. Cox, E. Vlieg, and I. K. Robinson, "Synchrotron Radiation Crystallography," Academic Press, London (1992).
19. J. E. Jaffe and A. Zunger, *Phys. Rev. B* **28,** 5822 (1983); *Phys. Rev. B* **29,** 1882 (1984).
20. S. C. Abrahams and J. L. Bernstein, *J. Chem. Phys.* **59,** 1625 (1973).
21. W. R. Busing and H. A. Levy, *Acta Crystallogr.* **22,** 457 (1967).
22. F. Frolow, private communication.
23. J. F. Nye, "Physical Properties of Crystals," 1st ed. Clarendon, Oxford (1957).
24. K. Ståhl, Å. Kvick, and S. C. Abrahams, *Acta Crystallogr. Sect. A* **46,** 478 (1990).
25. Y. Le Page, E. J. Gabe and G. J. Gainsford, *J. Appl. Crystallogr.* **23,** 406 (1990).
26. R. E. Newnham, private communication.
27. I. Fujimoto, *Jpn. J. Appl. Phys.* **19,** L347 (1980).
28. U. Pietsch, J. Mahlberg, and K. Unger, *Phys. Status Solidi B* **131,** 67 (1985).
29. W. H. Koschel and M. Bettini, *Phys. Status Solidi* **72,** 729 (1975).
30. G. D. Holah, J. S. Webb, and M. Montgomery, *J. Phys. C Solid State Phys.* **7,** 3875 (1974).
31. C.-C. Shih and A. Yariv, *J. Phys. C.* **15,** 825 (1982).
32. P. N. Keating, *Phys. Rev.* **145,** 637 (1966).
33. U. Schröder, *Solid State Commun.* **4,** 347 (1966).
34. K. Fischer, H. Bilz, R. Haberkorn, and W. Weber, *Phys. Status Solidi B* **54,** 285 (1972).
35. S. Fraga, J. Karwowski, and K. M. S. Saxena, "Handbook of Atomic Data, Elsevier: Amsterdam (1976).